NAROO program: Analysis of USNO Galilean observations 1967–1998

Vincent Robert-Pélissier, D. Pascu, V. Lainey, J.-E. Arlot

Icarus 426 (2025) 116344

Contents lists available at ScienceDirect

Icarus

journal homepage: www.elsevier.com/locate/icarus

Research Paper

NAROO program: Analysis of USNO Galilean observations 1967–1998

V. Robert [a,b,*], D. Pascu [c], V. Lainey [a], J.-E. Arlot [a]

[a] IMCCE, Observatoire de Paris, PSL Research University, CNRS UMR 8028, Sorbonne Universités, UPMC, Univ. Lille 1, 77 avenue Denfert-Rochereau, Paris 75014, France

[b] Institut Polytechnique des Sciences Avancées IPSA, 63 bis Boulevard de Brandebourg, Ivry-sur-Seine 94200, France

[c] U.S. Naval Observatory USNO (retired), 3450 Massachusetts Ave. NW, Washington, DC 20392, USA

ARTICLE INFO

Keywords:
Astrometry
Io
Europa
Ganymede
Callisto
Jupiter

ABSTRACT

The New Astrometric Reduction of Old Observations (NAROO) program is dedicated to the measurement of astrophotographic plates and the analysis of old observations for scientific purposes. One of the main objectives of the NAROO program is to provide accurate positional measurements of planets and satellites to improve our knowledge of their orbits and dynamics, and to infer the accuracy of the planet and satellite ephemerides. We digitized 553 astronegatives of the Galilean satellites taken with the McCormick 26-inch refractor in 1967/68 and the U.S. Naval Observatory 26-inch refractor from 1973 to 1998, resulting in 2650 individual observations. We measured and reduced these observations through an optimal process that includes image, instrumental, and spherical corrections using Gaia-DR3 catalog to provide the most accurate equatorial (RA, Dec) ICRS (Gaia-CRF3) positions. 4819 positions of the Galilean satellites have been determined with an accuracy of 55 mas (160 km at Jupiter), near the limit of the photographic technique for such work. These data can help to improve the equatorial positions of Jupiter. They also can be used in the context of quantifying tidal effects and will still be useful when Europa Clipper and Juice data will become available.

1. Introduction

The New Astrometric Reduction of Old Observations (NAROO) program has been developed as a unique center dedicated to the measurement of astrophotographic plates and the analysis of old observations for scientific purposes (Robert et al., 2021). The framework is the study of the dynamics of Solar System bodies, in particular, which require astrometric observations sampled over a long time span to quantify the long period terms that may help to analyze the evolution of the motion. One of the main objectives of the NAROO program is to provide accurate positional measurements of planets and satellites to improve our knowledge of their orbits and dynamics, and to infer the accuracy of the planet and satellite ephemerides.

We obtained the large photographic plate archive of the Galilean satellites taken at the McCormick Observatory in 1967/68 and the U. S. Naval Observatory (USNO) from 1973 to 1998 for remeasurement and reanalysis. These plates had been previously measured with the USNO automatic measuring machine, StarScan (Zacharias et al., 2008; Robert et al., 2016), reduced by the trail/scale scheme (Pascu, 1977) and used by Jet Propulsion Laboratory (JPL) for the navigation of the Voyager and Galileo space probes to successful reconnaissance with the Jovian system. However, three developments converged in the last decade to give the USNO plate archive new life and purpose. First, from theoretical studies at Institut de Mécanique Céleste et de Calcul des Éphémérides (IMCCE) in Paris, Desmars et al. (2009) have shown that astrometric data spread over a long time span were better than more accurate astrometric data spread over a short interval of time for dynamical and ephemeris purposes. Second, Arlot et al. (2012) have shown the benefit of using old observations and how new and future reductions with the Gaia catalog (Robin et al., 2012) will be useful and beneficial. And finally, the high precision NAROO measuring machine, superior to the StarScan, is now available for the community at Meudon (Robert et al., 2021). The expectation was that the astrometric positions of the planets, as well as the Galilean satellites, could now be obtained to the absolute limits of the photographic technique. Such old data remain extremely important for constraining the orbital dynamics of the Galilean system (Fayolle et al., 2023), in particular in the context of quantifying tidal effects.

2. Historical context

In 1610, Galileo discovered the four great moons of Jupiter, named for him. They are the brightest of the outer planetary satellites and can

* Corresponding author at: IMCCE, Observatoire de Paris, PSL Research University, CNRS UMR 8028, Sorbonne Universités, UPMC, Univ. Lille 1, 77 avenue Denfert- Rochereau, Paris 75014, France.

E-mail address: vincent.robert@obspm.fr (V. Robert).

https://doi.org/10.1016/j.icarus.2024.116344
Received 25 September 2024; Received in revised form 10 October 2024; Accepted 11 October 2024
Available online 22 October 2024

be seen by some sharp-eyed individuals with the unaided eye. Because of their brightness, they were both the most astrometrically observed and also by more varied techniques than any of the other planetary satellites.

Phenomena due to Jupiter, especially eclipses, were some of the earliest observations used for orbital correction because they could be made with small telescopes. Phenomena predictions were published in astronomical and navigational almanacs because they were used to correct chronometers used in navigation at sea, and land surveying. Notwithstanding their observational convenience, observations of phenomena relative to Jupiter were not the best for orbital correction. On any one night, few phenomena could be observed from any one site, and usually only for one satellite. Moreover, the observations were not well distributed around the orbit, indicating that some of the orbital parameters could not be determined well. For these reasons, observers favored tangent-plane observations which yielded positions for all four satellites at points well distributed around their orbits. The best of these early observations, according to de Sitter (1931), were the heliometer observations begun by Gill (1913) at the Cape in 1891.

Photographic observations of the Galileans were also begun very early — in the 1890s. Unfortunately, the instruments used were of short focal length and the results not competitive with the micrometer observations made with the visual long focus refractors. In discussing all modern observations of the Galileans made up to 1928, de Sitter (1931) concluded that the long focus photographic observations made by Alden and O'Connell (1928) at the Yale Southern Station at Johannesburg, South Africa, with their 26-inch photographic refractor in 1927 and 1928, were the most accurate. This conclusion was supported by the comparison made by Struve (1928) with his visual long focus micrometer observations.

3. USNO photographic observations

Following the 1967 IAU in Prague, Jean Kovalevsky, Director of the Bureau des Longitudes (BdL) in Paris, requested that the USNO obtain new astrometric observations of the Galilean satellites in order for BdL to update their ephemerides. The project was undertaken by Pascu (1977, 1979) in November of 1967, with the 26-inch refractor of the McCormick observatory of the University of Virginia (where he was a student). The McCormick refractor is a Clark refractor and a "twin" of the 26-inch refractor of the USNO. De Sitter's and Struve's conclusions informed the decision to adopt the long focus photographic technique for the observations. Plans were made to take photographic plates throughout the apparition of Jupiter, as the McCormick parallax program would allow, to cover long periodic terms, and to take plates intensively in order to cover the orbits well.

To reduce the brightness of Jupiter and the Galilean satellites, a special neutral filter was devised (Fig. 1). The filter was constructed from Kodak High Resolution Plates (HRP) and was composed of a central rectangle with dimensions to accommodate four to six exposures, spaced in declination, throughout the apparition, and three optical densities to produce a measurable image of Jupiter and to reduce the Galileans to 9th visual magnitude stars. This arrangement would not only reduce the random error due to seeing excursions by increasing the integration time, but would enable the determination of spherical equatorial coordinates for Jupiter from measurements on the planetary image, or if that proves not feasible, then indirectly from the satellites. Trails were taken nightly in case there was insufficient star coverage for a plate solution, and plates of the Praesepe and Pleiades star clusters were obtained occasionally to study the focal plane of the 26-inch. Since Jupiter and the Galileans would be in motion throughout the exposure, fast emulsions were required to record the faintest catalog stars in the shortest exposure. Kodak 103aG (antihalation backed), 5 × 7 × 0.06 inch plates were chosen after testing several emulsions. Plates were taken in combination with a Schott GG14 filter (yellow) in contact with the special filter. This combination filter was fixed in

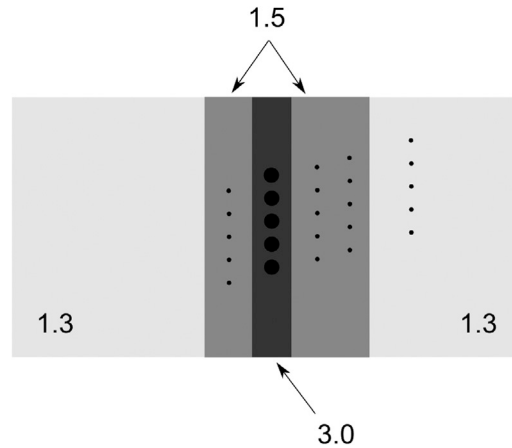

Fig. 1. Schematic of the special neutral filter used to produce a measurable image of Jupiter and to reduce the Galileans to 9th visual magnitude stars. The values 1.3, 1.5 and 3.0 denote the filter zonal densities.

a cartridge plate holder about 2 mm from the photographic emulsion. Four to six exposures, separated in declination, were taken per plate and ranged in duration from 20 to 40 s, depending on the transparency of the sky or the brightness of the catalog reference stars. Two or more plates were produced each night of observation. The UTC exposure start time was accurate to better than 0.5 s. A total of 293 exposures on 78 plates were taken on 31 nights over seven months.

No further plates were taken until 1973, at the request of NASA, to support the Voyager probes' reconnaissance of the outer planets. The Working Group of Outer Planet Satellites (Seidelmann, 1979), composed of international experts in astrometry and dynamics, was formed for the purpose of making recommendations to NASA for new ground based observations and theoretical work needed to improve the satellite ephemerides for the successful navigation of the Voyager probes to the outer planets. On the Working Group's recommendation, the USNO began a program of photographic astrometric observations of the Galilean satellite system with their 26-inch visual refractor (Pascu, 1977, 1979), while observations were continued at McCormick (Ianna and Seitzer, 1979), using the same techniques developed earlier, with one major exception. At the 1977/78 apparition, the USNO instrument was diaphragmed to 16 inches for one of the two plates taken each night. After that apparition, the USNO refractor was diaphragmed to 16 inches for the remainder of the observations. The purpose of the reduced aperture was to reduce coma to the corners of the plates, increasing the "coma-free" field, and thus, the number of usable catalog reference stars. The observations at USNO continued at every apparition of Jupiter until 1998, when Kodak discontinued their production of scientific plates, and the USNO supply of Kodak plates was depleted. Including the 1967/68 set of McCormick plates, the USNO archive of Galilean satellites observations numbers 683 multiple exposure plates, taken on 303 nights, 25 apparitions and over 31 years — more than two complete orbits of Jupiter around the Sun.

A particular attention has been paid to record the metadata over each plate envelope for use. Fig. 2 shows the information for the USNO Galilean plate No. 21014, which is a typical USNO envelope. One can clearly find all useful data: plate series and number in series, starting date and exposure time for all exposures, and some additional comments such as the material designation, the seeing criteria and the temperature.

4. Measurement and reduction

We selected 553 photographic plates from November 08, 1967 to December 09, 1998 to be transferred to Meudon and digitized with the

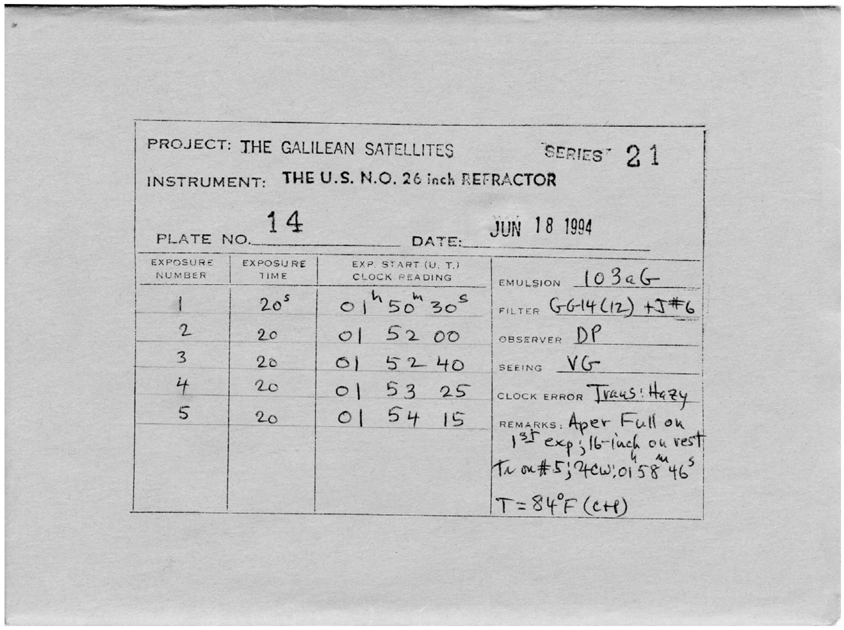

PROJECT: THE GALILEAN SATELLITES "SERIES" 21
INSTRUMENT: THE U.S. N.O. 26 inch REFRACTOR
PLATE NO. 14 DATE: JUN 18 1994

EXPOSURE NUMBER	EXPOSURE TIME	EXP. START (U. T.) CLOCK READING
1	20^s	$01^h 50^m 30^s$
2	20	01 52 00
3	20	01 52 40
4	20	01 53 25
5	20	01 54 15

EMULSION 103aG
FILTER GG14(12) +J#6
OBSERVER DP
SEEING VG
CLOCK ERROR Trans: Hazy
REMARKS: Aper Full on 1st exp; 16-inch on rest
Tr on #5; 4cw; $01^h 58^m 46^s$
T=84°F (c+l)

Fig. 2. Typical USNO photographic plate envelope with all information for astrometric measurement.

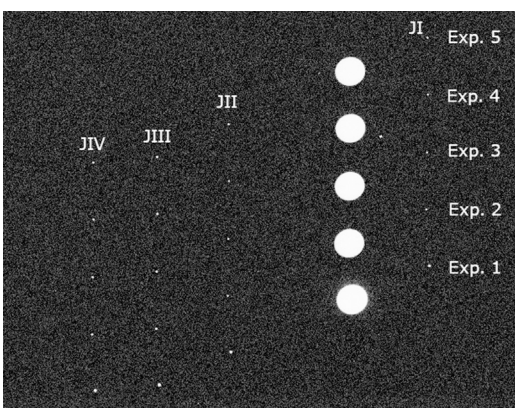

Fig. 3. Center of the digitization (positive) of the USNO 26-inch Galilean plate No. 21014. Five exposures shifted in the declination direction, from left to right: Callisto, Ganymede, Europa, Jupiter, and Io. North is up, east to the left.

NAROO machine. Each plate contains four to six exposures shifted in the declination direction. Most of the individual exposures were 20 s in duration with a few 30–40 s in poor transparency conditions. The field of view is 57 arcmin on the x-axis and 43 arcmin on the y-axis. Fig. 3 shows the center of the digitized (positive) USNO Galilean plate No. 21014, which is a typical digitized image. Five 20 s exposures of the Jovian system were taken with the USNO 26-inch refractor on 18 June 1994. Not visible in the figure, the small special filter covers the planet and satellites, reducing their light and providing a measurable image of Jupiter and the Galileans. From left to right, Callisto, Ganymede, Europa, Jupiter, and Io. North is up, east to the left.

Measured (x, y) plate positions were corrected for instrumental and spherical effects as described in Robert (2011), including corrections for the phase effect and the total chromatic atmospheric refraction. The plates contain 2 to as many as 67 reference stars, with an average of 6, and the reductions were performed using suitable four constant functional models to provide equatorial (RA, Dec) astrometric positions of the satellites. Scale ρ, orientation θ, and offsets Δx and Δy were modeled for the determination of the tangential (X, Y) coordinates. All our observations were equatorial (RA, Dec) astrometric positions obtained from tangential (X, Y) coordinates by using the gnomonic inverse projection, and determined in an ICRS (Gaia-CRF3) topocentric reference frame.

4.1. The telescope scale value and its temperature dependence

Since the plates with adequate reference star coverage were reduced by the method of plate constants, neither the plate scale nor its temperature variation were needed for the derivation of positional observations of the Galilean moons or of Jupiter. However, an accurate scale value would be useful to accurately reduce those plates which do not have sufficient reference star coverage for a plate constants reduction. The large plate archive, taken over more than 20 years, with a range in zenith distance of 50°, a temperature range over 35 °C and measured with high precision, on a high precision stellar grid, is uniquely suited for studies of the plate scale, its temperature variation and the stability of the 26-inch refractor at a diaphragmed 16-inch aperture.

Three factors contribute to the photographic plate scale of the telescope: the measuring machine used to measure the photographic plates, the atmosphere, and the temperature. The scale value was often identified with a specific measuring machine for the long screw machines, but the NAROO measuring machine is much more accurate, so this component is negligible. The atmosphere, due to refraction, contributes significantly to the scale value as a function of zenith distance (Van De Kamp, 1967). And the temperature affects the scale value, both due to its action on the telescope itself, and on the photographic plate. The effect of the atmosphere on the derived scale is to increase its numerical value with zenith distance, while the effect of increasing temperature on the telescope leads to a decrease in the numerical value. The effect of the temperature of the photographic glass plate is to increase the numerical value of the scale for temperatures higher than that at which the plates were measured, and decrease the numerical scale value at lower temperatures. The result of these opposing factors is to compensate for each other in most observations. This has been pointed out by McAlister et al. (1974) and according to them, the rationale for the practice of not changing the focus (for long focus refractors) with temperature as is the case for our USNO plate archive.

In our case, the atmospheric contribution to the plate scale compensates for the temperature contribution because the summer apparitions

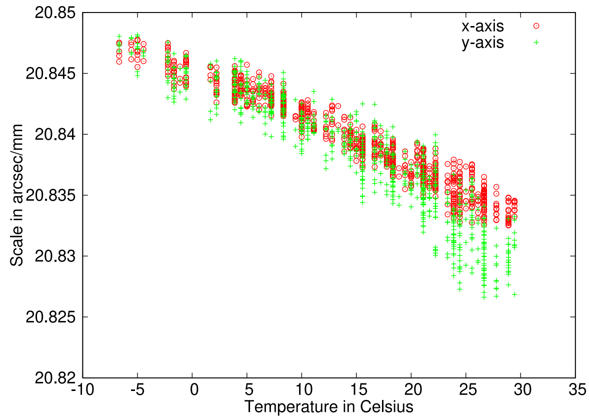

Fig. 4. Scale of the 26-inch refractor at a diaphragmed 16-inch aperture, outside the atmosphere in x-axis and y-axis from USNO observations, in function of the temperature during the observation.

were at the greatest zenith distances, while winter apparitions were at the smallest. For the 25-year span of this archive, Jupiter revolved around the sky twice. Because atmospheric refraction significantly affects the scale of the focal plane, correction for total refraction must have been be made. In fact, it had been done prior to the plate constants reductions using our model including the temperature parameter to compensate for the seasonal variation. The resulting temperature dependence of the scale of the 26-inch refractor, diaphragmed to 16-inch, is shown in Fig. 4. It is emphasized that this plot describes the dependence of the 26-inch telescope plate scale with temperature only outside of the atmosphere.

A determination can now be made for the contribution of the lens and/or the telescope tube to the plate scale. From Fig. 4, the scale at −5 °C is about 20.8455 arcsec/mm, corresponding to a focal length of 9894.94 mm. At 30 °C, the x-scale of 20.834 arcsec/mm corresponds to a focal length of 9900.40 mm. Thus, over the 35 °C range of the observations, the change in focal length was 5.5 mm. While an accurate value for the coefficient of thermal expansion for the 26-inch tube is not available, the range of values for steel is from 0.000011/°C to 0.000017/°C with a common value of 0.000012/°C, for a mean temperature of 20 °C at sea level. This value gives an expansion of the telescope tube as 4.2 mm over a temperature difference of 35 °C. With this approximation, it is evident that most, if not all, of the thermal contribution of the telescope to the plate scale is due to the lengthening of the steel telescope tube.

A puzzling feature of Fig. 4 is the deviation of the x and y scales at 24 °C. We have no explanation for this at this time. McAlister et al. (1974) found a similar result for the McCormick refractor but they also had no explanation for it and suggested that it could be due to flexure of the telescope tube. Such an explanation seems plausible for our situation since the deviation of the x and y scales occur at the greatest zenith distances. Presumably, the effect is similar to plate tilt and would result in a decrease in the numerical value of the y scale. In our result, the y scale is numerically decreased relative to the x scale at the greatest zenith distances. It is also possible that the standard refraction model corrections did not match well the atmospheric conditions at the largest zenith distances and highest temperatures.

4.2. Comparison NAROO vs. DAMIAN

Actually, we made a first analysis of these 553 photographic plates that were digitized, 13 years ago over 3 months, with the Digital Access to Metric Images Archives Network (DAMIAN) machine at the Royal Observatory of Belgium (de Cuyper et al., 2004; de Cuyper and Winter, 2005, 2006). Even if this previous analysis was valuable and the calculated positions used for the most recent IMCCE dynamical models (Robert, 2011; Robert et al., 2011), the results were never published. At this epoch, we were able to make measurements for 1071 positions of Io, 1122 positions of Europa, 1192 positions of Ganymede, and 1151 positions of Callisto. We focused on individual observations for which the residuals of the satellites were independently lower than the 3σ value of their rms residuals in right ascension and declination. We reduced the observations using the UCAC2 reference star catalog (Zacharias et al., 2004), and we compared the positions of the Galileans with their theoretical computed positions given by the INPOP10e planetary ephemeris (Fienga et al., 2013) and NOE-5-2010-JUP satellite ephemerides (Lainey et al., 2009). Much more recently, we digitized the 553 photographic plates with the NAROO machine, over 15 days, and we re-processed the analysis in exactly the same conditions of measurement, centroiding and reduction techniques using the UCAC2 reference star catalog, and the INPOP10e planetary ephemeris and NOE-5-2010-JUP satellite ephemerides for the comparison. Table 1 shows this new difference of (RA, Dec) coordinates for individual satellites, hence the observed positions versus positions calculated with NAROO digitizations.

Table 1
Details of the equatorial mean (O-C)s and residuals for the Galilean satellites in mas, according to NOE-5-2010-JUP and INPOP10e ephemerides, with NAROO digitizations.

Satellite	$\overline{(O-C)}_{\alpha\cos\delta}$	$\sigma_{\alpha\cos\delta}$	$\overline{(O-C)}_{\delta}$	σ_{δ}
JI	−5.0	63.6	−0.2	60.6
JII	−0.6	64.7	−1.0	60.9
JIII	−3.4	64.6	1.1	65.6
JIV	−0.8	63.0	−0.7	61.0
Average	−3.0	64.0	0.0	62.0

Residuals $\sigma_{\alpha\cos\delta}$ and σ_{δ} denote the overall accuracies for this 31-year observation set in right ascension and declination, respectively, assuming the comparison theories are definitive. Since we used the NAROO and DAMIAN machines to digitize twice the complete series in the same conditions of analysis, differences in results only reflect the quality of both digitizers. With regard to the differences between the average residuals on error contribution, we may conclude that the NAROO machine provides the best accuracy, and that the DAMIAN machine seems to be affected by a mean random error about of 6 mas, that is to say about of 300 nm. This value is nearly 4 times higher to that of 80 nm that we initially evaluated (Robert et al., 2011), but it is not inconsistent. The DAMIAN digitizations were made over 3 months and we learned, a posteriori, that the temperature of the machine clean room was not as stable as required because of technical issues. In nominal conditions, both instruments might be comparable. To avoid any compromise of the results, while digitizing with the NAROO machine, we ensure that the thermal enclosure of the digitizer meets all required conditions: overpressure ISO-5, temperature of 20 °C ± 0.1 °C and a relative humidity of 50% RH ± 5% RH. We use a thermal controller for this purpose before, during and after each digitization. Second, we control both the stability and repeatability of the machine before each scanning session, daily.

4.3. Positioning results

We finally re-processed the analysis of the 553 NAROO images using the Gaia-DR3 reference star catalog (Gaia Collaboration et al., 2016, 2023) to compare the positions of the Galilean satellites with their theoretical computed positions given by the INPOP21a planetary ephemeris (Fienga et al., 2021) and newest NOE-5-2021-JUP satellite ephemerides. All of the Gaia reference stars and the satellite images were centered using the shapelet decomposition method (Refregier, 2003), which is based on the linear decomposition of each object independently, in the images, into series of special basis functions of

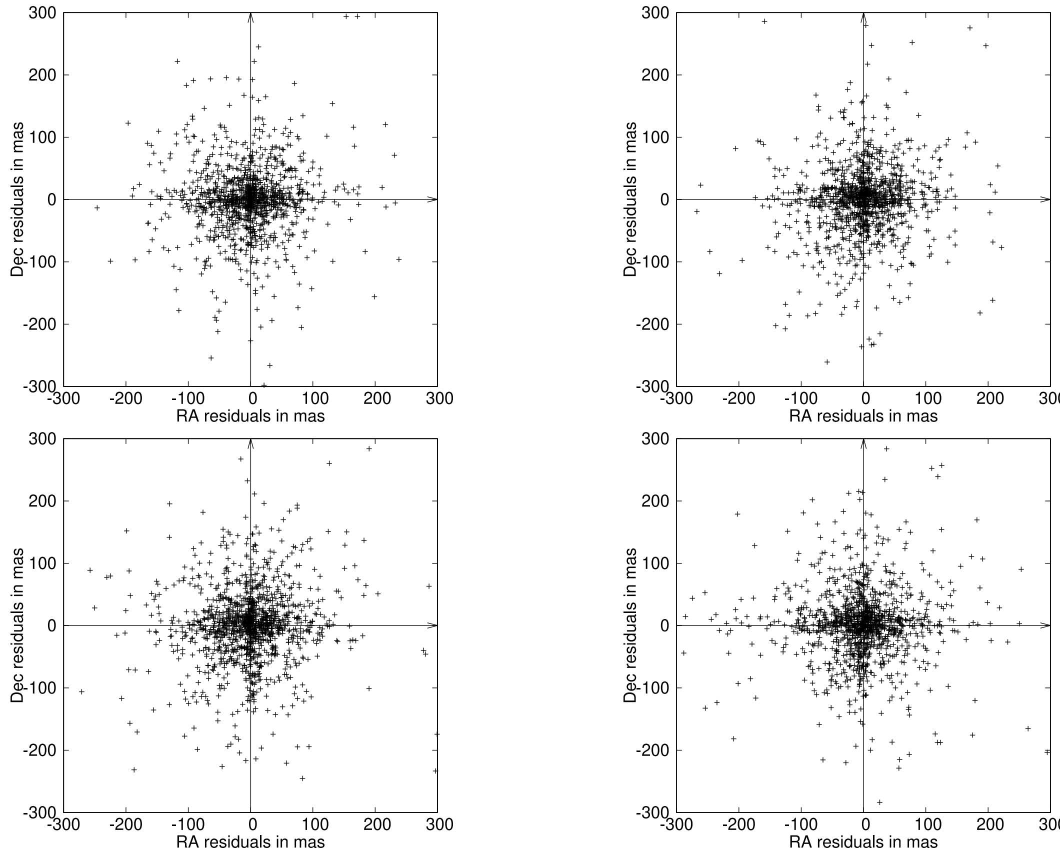

Fig. 5. Equatorial residuals according to NOE-5-2021-JUP and INPOP21a ephemerides. Starting from the top figure: Io (first), Europa (second), Ganymede (third) and Callisto (fourth). The x-axis shows the RA residuals and y-axis the Dec residuals.

Table 2
Extract from the astrometric positions list of the Galilean satellites available in electronic form at CDS via https://cdsarc.cds.unistra.fr/viz-bin/cat/VII/295 and IMCCE (http://nsdb.imcce.fr/nsdb/home.html).

Object	Date (TDB)	RA (deg.)	Dec (deg.)
Io	2 445 959.522154	274.164935	−23.488627
Europa	2 445 959.522154	274.133103	−23.491192
Ganymede	2 445 959.522154	274.220076	−23.487137
Callisto	2 445 959.522154	273.985602	−23.495681
Jupiter	2 445 959.522154	274.125929	−23.490659

different shapes. This concerns 1145 positions of Io, 1178 positions of Europa, 1274 positions of Ganymede, and 1222 positions of Callisto. We also computed 1355 positions of Jupiter as the barycenter of the observed satellites, when at least two of them were available on the same date. In the list available in electronic form at CDS via https://cdsarc.cds.unistra.fr/viz-bin/cat/VII/295 and IMCCE (http://nsdb.imcce.fr/nsdb/home.html), the corresponding topocentric observed positions refer to the ICRF, and the mean time of observation is given in Barycentric Dynamical Time TDB. Table 2 gives an extract of this list. Starting from the lefthand column, we provide the object name, the mean TDB date of observation in Julian Days, the topocentric observed right ascension, and declination in degrees. The distributions of the (O-C)s and residuals in equatorial right ascension and declination are provided in Figs. 5–6, and Table 3. They show the difference of (RA, Dec) coordinates for individual satellites, hence the observed positions versus positions calculated from INPOP21a and NOE-5-2021-JUP models with NAROO digitizations.

Offsets for each night of a single opposition are small and biases no longer occur in both the RA and Dec coordinates, using the Gaia-DR3 reference star catalog. By comparison with our former analysis using the UCAC2 reference star catalog (see Table 1), this indicates that Gaia-DR3 is not affected by local systematic errors (Robert et al., 2016). Offsets for each opposition set, visible in Fig. 6, are small, below 15 mas. Because these observations were not used in correcting the NOE-5-2021-JUP and INOPOP21a ephemerides, it could explain that some mean residuals do not include zero in error bars. Moreover and about the year 1980, several individual observations appear to be more diffuse on plates. This is confirmed by larger extraction errors, which could explain the systematic offsets in both right ascension and declination.

The average residuals for the observations made from 1967 to 1998 are very low in both coordinates. The satellite variances in RA are also higher than those in Dec, since their apparent motion is mainly in right ascension. Small systematic residuals also remain in this coordinate, within 2 mas of magnitude, which could be explained by two independent reasons. First, Perlbarg et al. (2023) simulated and estimated how a timing error at the minute-level could bias positioning results, mainly in the primary direction of the motion. Although, they concluded that timing error should now be included in dynamical adjustments while dealing with old observations. Second, we could consider deviations of the center of light in the satellite images from their geometric center due to surface variations, such as Io's volcanos for example, or due to large phase offsets. This is a problem that we are now able to detect since the diameters of the satellites are large relative to the observational errors. For phase offsets in right ascension, especially, the effect could be a problem because our observations are generally not evenly distributed around opposition. They were made for a longer period after opposition than before, due to weather and logistic reasons. These two causes are still being investigated with different and larger set of old observations.

To estimate the influence of the satellite ephemeris on the results, we computed the difference between observed positions and positions

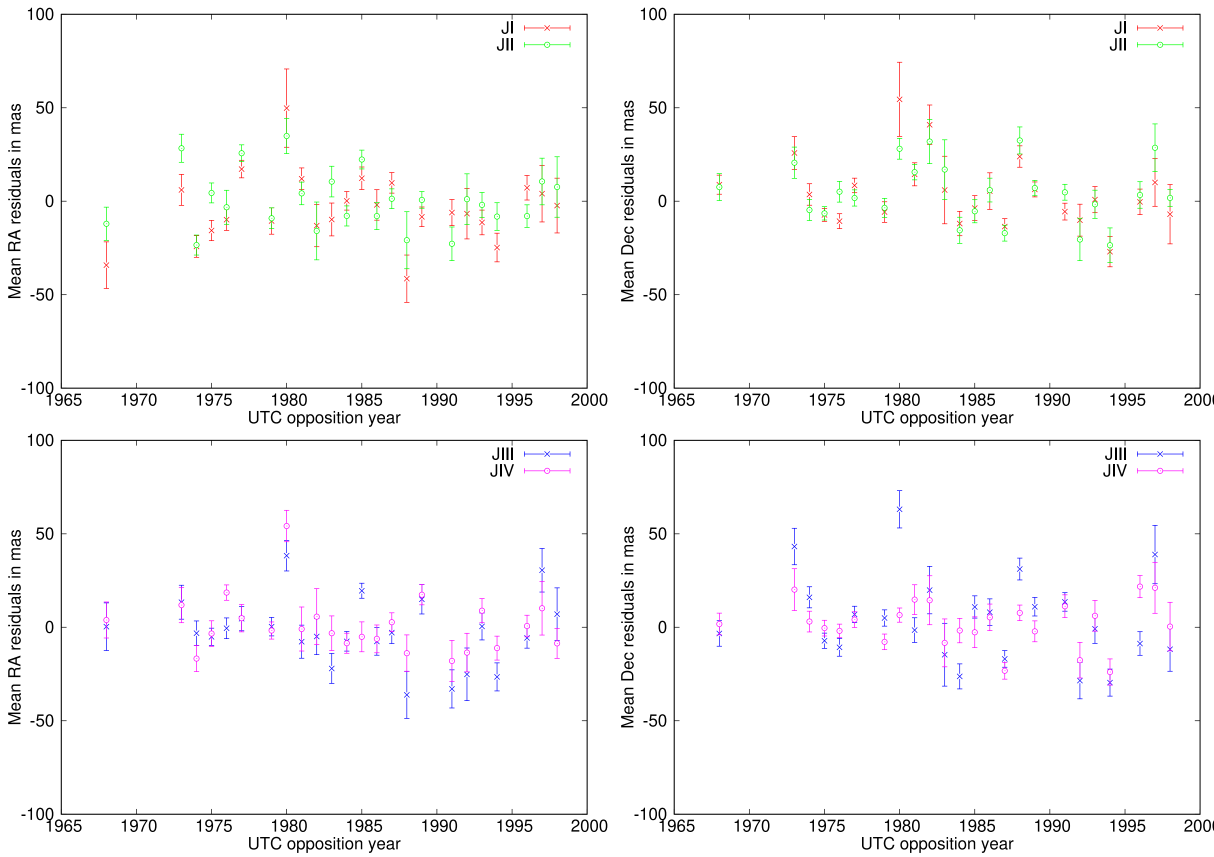

Fig. 6. Equatorial mean residuals according to NOE-5-2021-JUP and INPOP21a ephemerides. The x-axis shows the UTC year of opposition and y-axis the RA and Dec mean residuals with errors.

Table 3
Details of the equatorial mean (O-C)s and residuals for the Galilean satellites in mas, according to NOE-5-2021-JUP and INPOP21a ephemerides, with NAROO digitizations. SEM denotes the Standard Error of the Mean as a criteria of accuracy for the mean individual (O-C)s.

Satellite	$\overline{(O-C)}_{\alpha\cos\delta}$	$SEM_{\alpha\cos\delta}$ +/−	$\sigma_{\alpha\cos\delta}$ +/−	$\overline{(O-C)}_{\delta}$	SEM_{δ} +/−	σ_{δ} +/−
JI	−4.8	1.6	55.7	0.3	1.5	52.5
JII	−0.5	1.5	53.3	−0.1	1.5	52.7
JIII	−2.4	1.6	57.0	1.0	1.6	57.4
JIV	−1.0	1.6	56.2	0.9	1.5	52.5
Average	−2.1	0.8	55.6	0.5	0.8	53.9

Table 4
Details of the equatorial mean (O-C)s and residuals for the Galilean satellites in mas, according to JUP365 and INPOP21a ephemerides, with NAROO digitizations.

Satellite	$\overline{(O-C)}_{\alpha\cos\delta}$	$\sigma_{\alpha\cos\delta}$	$\overline{(O-C)}_{\delta}$	σ_{δ}
JI	−4.7	54.7	0.3	52.1
JII	−3.3	54.4	−0.1	52.9
JIII	−2.0	57.4	1.0	57.8
JIV	1.0	57.2	0.0	52.1
Average	−2.1	56.0	0.3	53.8

calculated from the current exportable JUP365 JPL ephemerides, and results are very similar, as expected. For individual satellites, the maximum difference is below 0.2 mas on their averaged (O-C)s, and below 0.4 mas on their overall accuracies. The typical differences between JUP365 and NOE-5-2021 are a few tens of kilometers, and those differences tend to vanish when moons are close to elongation. The fact that both ephemerides provide the same statistics suggests that their accuracy is similar. Table 4 shows the difference between the observed positions and positions calculated from JUP365 ephemerides.

The key point is that the NOE-5-2021-JUP/INPOP21a rms (O-C) for all observations is 54.1 mas for Io, 53.0, mas for Europa, 57.2 mas for Ganymede, and 54.3 mas for Callisto. These average rms (O-C)s correspond to our observation accuracies over twenty-six oppositions in the series, or 31 years. Centering all the Gaia reference stars and the satellite images using the shapelet decomposition method helped us to decrease the residuals by about of 1.5 mas in both right ascension and declination, by comparison to our former analysis (see Table 1). But the main improvement consisted in using the Gaia-DR3 star catalog for the positioning of the stellar references for the astrometric reduction. In fact, we were able to decrease the residuals by about of 7 mas in both right ascension and declination, by comparison to our former analysis. With regard to the differences between the average residuals, we may conclude that we eliminated an error contribution about of 28 mas, indicating that our first measurements were degraded by unmodeled uncertainties. This result is consistent with the expected mean error of 15–30 mas of the UCAC2 catalog (Zacharias et al., 2008), and we may deduce that the error contribution of the Gaia DR3 catalog is negligible for our needs, as expected.

First, our observations are original since they were not used in any planetary model. Such data can help to improve the equatorial positions of Jupiter and, thus, Jupiter's orbit more than twice around the sky. Second, as mentioned in Lainey et al. (2009) and more recently in Fayolle et al. (2023), classical astrometry remains extremely important for constraining the orbital dynamics of the Galilean system. Indeed, these data are particularly relevant in the context of quantifying tidal effects. Moreover, as Fayolle et al. (2023) have shown, NAROO data will still be useful when Europa Clipper and Juice data will become available.

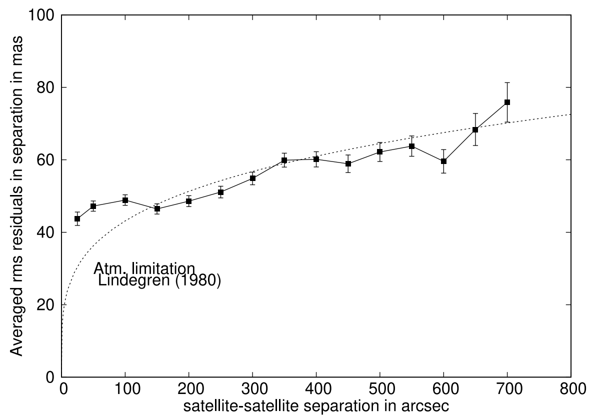

Fig. 7. Averaged rms residuals in the (satellite-satellite) separations according to NOE-5-2021-JUP ephemerides. The x-axis shows the satellite-satellite separation and the y-axis the averaged rms residuals in separation. Atmospheric limitation is given by Lindegren (1980).

Table 5
Comparison of the mass of Amalthea estimated with NAROO digitizations, and the one calculated from Galileo flybys by Anderson et al. (2005).

Source	Amplitude (km)	Mass (.10^{18} kg)
USNO plates	20.00 ± 2	2.00 ± 0.20
Galileo	–	2.08 ± 0.15

4.4. Intersatellite results

The best way to estimate the accuracy of our observations and how close it is to the limit of the photographic technique is to assess the accuracy of the intersatellite data because the differential positions (one satellite relative to another) minimize systematic errors such as phase effects and image motion, and allow us to eliminate the contribution of the planetary model errors on the residuals too. To assess the accuracy of the intersatellite observations, we compared our residuals to the accuracy limit imposed by the random seeing excursions. For that, we used the formulation proposed by Lindegren (1980) in which the expected mean error is directly proportional to the (0.25) power of the satellites' separation, S, in radians and inversely proportional to the (0.5) power of the integration time, T, exposure time in seconds. In Fig. 7, we plotted our mean rms residuals in intersatellite separation, relative to NOE-5-2021-JUP computed positions, against the mean satellite separations (6 combinations). For comparison, we also plotted Lindegren's function for 20 s exposures — the integration time for most of the observations.

The figure shows that our observations closely track Lindegren's relation between 150 and 700 arcsec separations. Since NOE-5-2021-JUP is a definitive theory, we may conclude that we have reached the seeing limit in accuracy in the 150 to 700 arcsec separation range. In addition, any systematic error remaining in the intersatellite separations, is below detection above the seeing random contribution. Short of 150 arcsec separations, however, the observational errors do not drop off nearly as much as expected as separations approach the size of the isoplanatic patch. Though the error does decrease to about 42 mas, some small systematic errors are possible in this separation range. Separations below about 1 mm on the photographic plate are problematic due to the Kostinsky effect (Kostinsky, 1908) and there may also be issues with measurement of close images. Further investigation to resolve these problems continues. While we expected some improvement on NOE-5-2021-JUP using Gaia-DR3 reference star catalog, the main improvement will be in the equatorial positions of Jupiter and, thus, the improvement of Jupiter's orbit.

4.5. The case of Amalthea

Amalthea (JV) is one of the four inner satellites of Jupiter with Metis (JXVI), Adrastea (JXV) and Thebe (JXIV). These bodies all have an irregular shape, their orbits are weakly eccentric, and they interact with Jupiter's rings (Ockert-Bell et al., 1999). Amalthea is the largest and the most massive. Because of their small sizes and albedos, they are difficult to observe from Earth. Only Amalthea was discovered by Barnard in 1892 from ground. Metis, Adrastea and Thebe were discovered thanks to Voyager images.

We compared the positions of the Galilean satellites with their theoretical computed positions given by the INPOP21a planetary ephemeris and former NOE-5-2010-JUP satellite ephemerides. In fact and by its definition, NOE-5-2010-JUP satellite model did not introduce the motion of the inner satellites. Their influence was taken into account by adding their mass to that of Jupiter. Thus, considering that Io is the main Galilean disturbed by the gravitational potential of the inners, we should be able to detect such an additional signal in its (O-C)s, in particular. To do so, we performed a frequency analysis of these data normalized by the Earth/satellite distance to reduce extra signals (motion of the observer, planetary ephemeris...) over 31 years, at the known frequencies of the four inner satellites. We assumed that the measured signals corresponded to variations in longitude since we were looking for mass estimations. Therefore, we were able to extract a 0.5016 ± 0.0022-days periodic signal of 20 ± 2 km of magnitude for the argument $\lambda_{JV} - \lambda_{JI}$.

As a first approximation, we consider Amalthea as a perturber in the (Jupiter;Io) 2-body system. We also assume the problem in a single plane, with circular orbits. Then, following a simple analytical development of the corresponding disturbing function, we easily show that the periodic variation in the longitude of Io, at the first order, is given by:

$$\Delta L_1 = \frac{4\mu a}{n_I a_I^4 (n - n_I)} \sin(M - M_I) = \breve{A} \cdot \sin(M - M_I)$$

With $\mu = GM_J$ the central potential of Jupiter, a_I and n_I the mean semi-major axis and mean motion of Io, respectively, a and n the mean semi-major axis and mean motion of Amalthea, respectively, $(M - M_I)$ the periodic argument of the variation in longitude on Io. $\breve{A}$ is finally the signal amplitude to compare to that we detected, after a correction by a a_I^2/d factor with d the mean Earth-Io distance to express the angle variation in km on the celestial sphere.

Table 5 shows the comparison between the mass of Amalthea we estimated from our observations, and the mass of Amalthea that was calculated from Galileo flybys by Anderson et al. (2005). Both results are in the same order of magnitude. The differences are mainly due to the hypotheses of our estimation method, and to the mean values of a_I, n_I and a we used. Although, our measuring error is a resulting indicator of these uncertainties. The key point is that we confirm that direct observation is not the only way to determine the physical characteristics of celestial bodies, and a new analysis of photographic plates could help to get more information about various bodies to contribute to a more fundamental physics.

5. Summary and future work

We analyzed a full series of astrophotographic plates of the Galilean satellites taken with the McCormick and USNO 26-inch refractors from 1967 to 1998. Using the NAROO machine for the digitization and the Gaia-DR3 reference star catalog allowed us to increase the precision and more important, to approach the limit of astrometric accuracy of the photographic technique for such work. Thus, we were able to provide astrometric (RA, Dec) ICRS (Gaia-CRF3) positions of the satellites, allowing us to deduce positions of the planet indirectly, with overall rms residuals of about 55 mas or 160 km at Jupiter. These observations will obviously be used to correct the forthcoming IMCCE dynamical models of Jupiter and the Galileans. We also showed that such observations could contribute to a more fundamental physics by estimating, indirectly, the mass of a gravitational perturber in the case of Amalthea.

Our data can help to improve the equatorial positions of Jupiter and, thus, Jupiter's orbit more than twice around the sky. They also can be used in the context of quantifying tidal effects since classical astrometry remains extremely important for constraining the orbital dynamics of the Galilean system. Moreover, NAROO data will still be useful when Europa Clipper and Juice data will become available.

We therefore confirm the high interest in continuing the analysis of old observations, especially photographic plates, in the framework of the NAROO program. Our team is focused on various projects now dealing with collections of Saturnian plates and Uranian plates that will help to improve the dynamics of corresponding systems. Since digitization time is reserved for external users, we remind all that the NAROO machine is available for researchers to digitize their own collections following our call for proposals, issued every six months via our project website.[1]

CRediT authorship contribution statement

V. Robert: Writing – review & editing, Writing – original draft, Visualization, Validation, Supervision, Software, Resources, Project administration, Methodology, Investigation, Formal analysis, Data curation, Conceptualization. **D. Pascu:** Validation, Investigation, Formal analysis, Conceptualization. **V. Lainey:** Validation, Investigation, Conceptualization. **J.-E. Arlot:** Validation, Investigation, Conceptualization.

Declaration of competing interest

The authors declare that they have no known competing financial interests or personal relationships that could have appeared to influence the work reported in this paper.

Acknowledgments

The NAROO program was supported by the DIM-ACAV of Île-de-France region, PSL Research University, the Programme National GRAM (PNGRAM), the Programme National de Planétologie (PNP) and the Programme National Soleil-Terre (PNST) of CNRS/INSU with INP and IN2P3, co-funded by CNES, and the Gaia Specific Action (AF Gaia) of Paris Observatory. This work has made use of data from the European Space Agency (ESA) mission *Gaia* (https://www.cosmos.esa.int/gaia), processed by the *Gaia* Data Processing and Analysis Consortium (DPAC, https://www.cosmos.esa.int/web/gaia/dpac/consortium). Funding for the DPAC has been provided by national institutions, in particular the institutions participating in the *Gaia* Multilateral Agreement.

Data availability

Positional data available at NSDB and CDS services.

[1] NAROO webpage https://naroo.imcce.fr/.

References

Alden, H.L., O'Connell, W., 1928. Photographic measures of the satellites of Saturn in 1926. Astron. J. 38, 53–56. http://dx.doi.org/10.1086/104808.

Anderson, J.D., Johnson, T.V., Schubert, G., Asmar, S., Jacobson, R.A., Johnston, D., Lau, E.L., Lewis, G., Moore, W.B., Taylor, A., Thomas, P.C., Weinwurm, G., 2005. Amalthea's density is less than that of water. Science 308 (5726), 1291–1293. http://dx.doi.org/10.1126/science.1110422.

Arlot, J.-E., Desmars, J., Lainey, V., Robert, V., 2012. The astrometry of the natural planetary satellites applied to their dynamics before and after Gaia. Planet. Space Sci. 73 (1), 66–69. http://dx.doi.org/10.1016/j.pss.2012.10.002.

de Cuyper, J., Winter, L., 2005. The D4A digitiser. In: Shopbell, P., Britton, M., Ebert, R. (Eds.), Astronomical Data Analysis Software and Systems XIV. In: Astronomical Society of the Pacific Conference Series, vol. 347, p. 651.

de Cuyper, J.P., Winter, L., 2006. The D4A digitiser. In: Gabriel, C., Arviset, C., Ponz, D., Enrique, S. (Eds.), Astronomical Data Analysis Software and Systems XV. In: Astronomical Society of the Pacific Conference Series, vol. 351, p. 587.

de Cuyper, J.P., Winter, L., Vanommeslaeghe, J., 2004. The D4A digitiser. In: Ochsenbein, F., Allen, M.G., Egret, D. (Eds.), Astronomical Data Analysis Software and Systems (ADASS) XIII. In: Astronomical Society of the Pacific Conference Series, vol. 314, p. 77.

de Sitter, W., 1931. Jupiter's Galilean satellites (george darwin lecture). Mon. Not. R. Astron. Soc. 91, 706–738. http://dx.doi.org/10.1093/mnras/91.7.706.

Desmars, J., Arlot, S., Arlot, J.E., Lainey, V., Vienne, A., 2009. Estimating the accuracy of satellite ephemerides using the bootstrap method. Astron. Astrophys. 499 (1), 321–330. http://dx.doi.org/10.1051/0004-6361/200811509.

Fayolle, M., Magnanini, A., Lainey, V., Dirkx, D., Zannoni, M., Tortora, P., 2023. Combining astrometry and JUICE - Europa Clipper radio science to improve the ephemerides of the Galilean moons. Astron. Astrophys. 677, A42. http://dx.doi.org/10.1051/0004-6361/202347065, arXiv:2307.15966.

Fienga, A., Deram, P., Di Ruscio, A., Viswanathan, V., Camargo, J.I.B., Bernus, L., Gastineau, M., Laskar, J., 2021. INPOP21a Planetary Ephemerides. Vol. 110, Notes Scientifiques et Techniques de l'Institut de Mecanique Celeste.

Fienga, A., Manche, H., Laskar, J., Gastineau, M., Verma, A., 2013. INPOP new release: INPOP10e. http://dx.doi.org/10.48550/arXiv.1301.1510, arXiv e-prints, arXiv:1301.1510.

Gaia Collaboration, Prusti, T., de Bruijne, J.H.J., Brown, A.G.A., Vallenari, A., Babusiaux, C., Bailer-Jones, C.A.L., Bastian, U., Biermann, M., Evans, D.W., Eyer, L., Jansen, F., Jordi, C., Klioner, S.A., Lammers, U., Lindegren, L., Luri, X., Mignard, F., Milligan, D.J., Panem, C., Poinsignon, V., Pourbaix, D., Randich, S., Sarri, G., Sartoretti, P., Siddiqui, H.I., Soubiran, C., Valette, V., van Leeuwen, F., Walton, N.A., Aerts, C., Arenou, F., Cropper, M., Drimmel, R., Høg, E., Katz, D., Lattanzi, M.G., O'Mullane, W., Grebel, E.K., Holland, A.D., Huc, C., Passot, X., Bramante, L., Cacciari, C., Castañeda, J., Chaoul, L., Cheek, N., De Angeli, F., Fabricius, C., Guerra, R., Hernández, J., Jean-Antoine-Piccolo, A., Masana, E., Messineo, R., Mowlavi, N., Nienartowicz, K., Ordóñez-Blanco, D., Panuzzo, P., Portell, J., Richards, P.J., Riello, M., Seabroke, G.M., Tanga, P., Thévenin, F., Torra, J., Els, S.G., Gracia-Abril, G., Comoretto, G., Garcia-Reinaldos, M., Lock, T., Mercier, E., Altmann, M., Andrae, R., Astraatmadja, T.L., Bellas-Velidis, I., Benson, K., Berthier, J., Blomme, R., Busso, G., Carry, B., Cellino, A., Clementini, G., Cowell, S., Creevey, O., Cuypers, J., Davidson, M., De Ridder, J., de Torres, A., Delchambre, L., Dell'Oro, A., Ducourant, C., Frémat, Y., García-Torres, M., Gosset, E., Halbwachs, J.L., Hambly, N.C., Harrison, D.L., Hauser, M., Hestroffer, D., Hodgkin, S.T., Huckle, H.E., Hutton, A., Jasniewicz, G., Jordan, S., Kontizas, M., Korn, A.J., Lanzafame, A.C., Manteiga, M., Moitinho, A., Muinonen, K., Osinde, J., Pancino, E., Pauwels, T., Petit, J.M., Recio-Blanco, A., Robin, A.C., Sarro, L.M., Siopis, C., Smith, M., Smith, K.W., Sozzetti, A., Thuillot, W., van Reeven, W., Viala, Y., Abbas, U., Abreu Aramburu, A., Accart, S., Aguado, J.J., Allan, P.M., Allasia, W., Altavilla, G., Álvarez, M.A., Alves, J., Anderson, R.I., Andrei, A.H., Anglada Varela, E., Antiche, E., Antoja, T., Antón, S., Arcay, B., Atzei, A., Ayache, L., Bach, N., Baker, S.G., Balaguer-Núñez, L., Barache, C., Barata, C., Barbier, A., Barblan, F., Baroni, M., Barrado y Navascués, D., Barros, M., Barstow, M.A., Becciani, U., Bellazzini, M., Bellei, G., Bello García, A., Belokurov, V., Bendjoya, P., Berihuete, A., Bianchi, L., Bienaymé, O., Billebaud, F., Blagorodnova, N., Blanco-Cuaresma, S., Boch, T., Bombrun, A., Borrachero, R., Bouquillon, S., Bourda, G., Bouy, H., Bragaglia, A., Breddels, M.A., Brouillet, N., Brüsemeister, T., Bucciarelli, B., Budnik, F., Burgess, P., Burgon, R., Burlacu, A., Busonero, D., Buzzi, R., Caffau, E., Cambras, J., Campbell, H., Cancelliere, R., Cantat-Gaudin, T., Carlucci, T., Carrasco, J.M., Castellani, M., Charlot, P., Charnas, J., Charvet, P., Chassat, F., Chiavassa, A., Clotet, M., Cocozza, G., Collins, R.S., Collins, P., Costigan, G., Crifo, F., Cross, N.J.G., Crosta, M., Crowley, C., Dafonte, C., Damerdji, Y., Dapergolas, A., David, P., David, M., De Cat, P., de Felice, F., de Laverny, P., De Luise, F., De March, R., de Martino, D., de Souza, R., Debosscher, J., del Pozo, E., Delbo, M., Delgado, A., Delgado, H.E., di Marco, F., Di Matteo, P., Diakite, S., Distefano, E., Dolding, C., Dos Anjos, S., Drazinos, P., Durán, J., Dzigan, Y., Ecale, E., Edvardsson, B., Enke, H., Erdmann, M., Escolar, D., Espina, M., Evans, N.W., Eynard Bontemps, G., Fabre, C., Fabrizio, M., Faigler, S., Falcão, A.J., Farràs Casas, M., Faye, F., Federici, L., Fedorets, G., Fernández-Hernández, J., Fernique, P., Fienga, A., Figueras, F., Filippi, F., Findeisen, K., Fonti, A., Fouesneau, M., Fraile, E., Fraser, M., Fuchs, J., Furnell, R., Gai, M., Galleti, S., Galluccio, L., Garabato, D., García-Sedano, F., Garé, P., Garofalo, A., Garralda, N., Gavras, P., Gerssen, J., Geyer, R., Gilmore, G., Girona, S., Giuffrida, G., Gomes, M., González-Marcos, A., González-Núñez, J., González-Vidal, J.J., Granvik, M., Guerrier, A., Guillout, P., Guiraud, J., Gúrpide, A., Gutiérrez-Sánchez, R., Guy, L.P., Haigron, R., Hatzidimitriou, D., Haywood, M., Heiter, U., Helmi, A., Hobbs, D., Hofmann, W., Holl, B., Holland, G., Hunt, J.A.S., Hypki, A., Icardi, V., Irwin, M., Jevardat de Fombelle, G., Jofré, P., Jonker, P.G., Jorissen, A., Julbe, F., Karampelas, A., Kochoska, A., Kohley, R., Kolenberg, K., Kontizas, E., Koposov, S.E., Kordopatis, G., Koubsky, P., Kowalczyk, A., Krone-Martins, A., Kudryashova, M., Kull, I., Bachchan, R.K., Lacoste-Seris, F., Lanza, A.F., Lavigne, J.B., Le Poncin-Lafitte, C., Lebreton, Y., Lebzelter, T., Leccia, S., Leclerc, N., Lecoeur-Taibi, I., Lemaitre, V., Lenhardt, H., Leroux, F., Liao, S., Licata, E., Lindstrøm, H.E.P., Lister, T.A., Livanou, E., Lobel, A., Löffler, W., López, M., Lopez-Lozano, A., Lorenz, D., Loureiro, T., MacDonald, I., Magalhães Fernandes, T., Managau, S., Mann, R.G., Mantelet, G., Marchal, O., Marchant, J.M., Marconi, M., Marie, J., Marinoni, S., Marrese, P.M., Marschalkó, G., Marshall, D.J., Martín-Fleitas, J.M., Martino, M., Mary, N., Matijevič, G., Mazeh, T., McMillan, P.J., Messina, S., Mestre, A., Michalik, D., Millar, N.R., Miranda, B.M.H., Molina, D., Molinaro, R., Molinaro, M., Molnár, L., Moniez, M., Montegriffo, P., Monteiro, D., Mor, R., Mora, A., Morbidelli, R., Morel, T., Morgenthaler, S., Morley, T., Morris, D., Mulone, A.F., Muraveva, T., Musella, I., Narbonne, J., Nelemans, G., Nicastro, L., Noval, L., Ordénovic, C., Ordieres-Meré, J., Osborne, P., Pagani, C., Pagano, I., Pailler, F., Palacin, H., Palaversa, L., Parsons, P., Paulsen, T., Pecoraro, M., Pedrosa, R., Pentikäinen, H., Pereira, J., Pichon, B., Piersimoni, A.M., Pineau, F.X., Plachy, E., Plum, G., Poujoulet, E., Prša, A., Pulone, L., Ragaini, S., Rago, S., Rambaux, N., Ramos-Lerate, M., Ranalli, P., Rauw, G., Read, A., Regibo, S., Renk, F., Reylé, C., Ribeiro, R.A., Rimoldini, L., Ripepi, V., Riva, A., Rixon, G., Roelens, M., Romero-Gómez, M., Rowell, N., Royer, F., Rudolph, A., Ruiz-Dern, L., Sadowski, G., Sagristà Sellés, T., Sahlmann, J., Salgado, J., Salguero, E., Sarasso, M., Savietto, H., Schnorhk, A., Schultheis, M., Sciacca, E., Segol, M., Segovia, J.C., Segransan, D., Serpell, E., Shih, I.C., Smareglia, R., Smart, R.L., Smith, C., Solano, E., Solitro, F., Sordo, R., Soria Nieto, S., Souchay, J., Spagna, A., Spoto, F., Stampa, U., Steele, I.A., Steidelmüller, H., Stephenson, C.A., Stoev, H., Suess, F.F., Süveges, M., Surdej, J., Szabados, L., Szegedi-Elek, E., Tapiador, D., Taris, F., Tauran, G., Taylor, M.B., Teixeira, R., Terrett, D., Tingley, B., Trager, S.C., Turon, C., Ulla, A., Utrilla, E., Valentini, G., van Elteren, A., Van Hemelryck, E., van Leeuwen, M., Varadi, M., Vecchiato, A., Veljanoski, J., Via, T., Vicente, D., Vogt, S., Voss, H., Votruba, V., Voutsinas, S., Walmsley, G., Weiler, M., Weingrill, K., Werner, D., Wevers, T., Whitehead, G., Wyrzykowski, Ł., Yoldas, A., Žerjal, M., Zucker, S., Zurbach, C., Zwitter, T., Alecu, A., Allen, M., Allende Prieto, C., Amorim, A., Anglada-Escudé, G., Arsenijevic, V., Azaz, S., Balm, P., Beck, M., Bernstein, H.H., Bigot, L., Bijaoui, A., Blasco, C., Bonfigli, M., Bono, G., Boudreault, S., Bressan, A., Brown, S., Brunet, P.M., Bunclark, P., Buonanno, R., Butkevich, A.G., Carret, C., Carrion, C., Chemin, L., Chéreau, F., Corcione, L., Darmigny, E., de Boer, K.S., de Teodoro, P., de Zeeuw, P.T., Delle Luche, C., Domingues, C.D., Dubath, P., Fodor, F., Frézouls, B., Fries, A., Fustes, D., Fyfe, D., Gallardo, E., Gallegos, J., Gardiol, D., Gebran, M., Gomboc, A., Gómez, A., Grux, E., Gueguen, A., Heyrovsky, A., Hoar, J., Iannicola, G., Isasi Parache, Y., Janotto, A.M., Joliet, E., Jonckheere, A., Keil, R., Kim, D.W., Klagyivik, P., Klar, J., Knude, J., Kochukhov, O., Kolka, I., Kos, J., Kutka, A., Lainey, V., LeBouquin, D., Liu, C., Loreggia, D., Makarov, V.V., Marseille, M.G., Martayan, C., Martinez-Rubi, O., Massart, B., Meynadier, F., Mignot, S., Munari, U., Nguyen, A.T., Nordlander, T., Ocvirk, P., O'Flaherty, K.S., Olias Sanz, A., Ortiz, P., Osorio, J., Oszkiewicz, D., Ouzounis, A., Palmer, M., Park, P., Pasquato, E., Peltzer, C., Peralta, J., Péturaud, F., Pieniluoma, T., Pigozzi, E., Poels, J., Prat, G., Prod'homme, T., Raison, F., Rebordao, J.M., Risquez, D., Rocca-Volmerange, B., Rosen, S., Ruiz-Fuertes, M.I., Russo, F., Sembay, S., Serraller Vizcaino, I., Short, A., Siebert, A., Silva, H., Sinachopoulos, D., Slezak, E., Soffel, M., Sosnowska, D., Straižys, V., ter Linden, M., Terrell, D., Theil, S., Tiede, C., Troisi, L., Tsalmantza, P., Tur, D., Vaccari, M., Vachier, F., Valles, P., Van Hamme, W., Veltz, L., Virtanen, J., Wallut, J.M., Wichmann, R., Wilkinson, M.I., Ziaeepour, H., Zschocke, S., 2016. The Gaia mission. Astron. Astrophys. 595, A1. http://dx.doi.org/10.1051/0004-6361/201629272, arXiv:1609.04153.

Gaia Collaboration, Vallenari, A., Brown, A.G.A., Prusti, T., de Bruijne, J.H.J., Arenou, F., Babusiaux, C., Biermann, M., Creevey, O.L., Ducourant, C., Evans, D.W., Eyer, L., Guerra, R., Hutton, A., Jordi, C., Klioner, S.A., Lammers, U.L., Lindegren, L., Luri, X., Mignard, F., Panem, C., Pourbaix, D., Randich, S., Sartoretti, P., Soubiran, C., Tanga, P., Walton, N.A., Bailer-Jones, C.A.L., Bastian, U., Drimmel, R., Jansen, F., Katz, D., Lattanzi, M.G., van Leeuwen, F., Bakker, J., Cacciari, C., Castañeda, J., De Angeli, F., Fabricius, C., Fouesneau, M., Frémat, Y., Galluccio, L., Guerrier, A., Heiter, U., Masana, E., Messineo, R., Mowlavi, N., Nicolas, C., Nienartowicz, K., Pailler, F., Panuzzo, P., Riclet, F., Roux, W., Seabroke, G.M., Sordo, R., Thévenin, F., Gracia-Abril, G., Portell, J., Teyssier, D., Altmann, M., Andrae, R., Audard, M., Bellas-Velidis, I., Benson, K., Berthier, J., Blomme, R., Burgess, P.W., Busonero, D., Busso, G., Cánovas, H., Carry, B., Cellino, A., Cheek, N., Clementini, G., Damerdji, Y., Davidson, M., de Teodoro, P., Nuñez Campos, M., Delchambre, L., Dell'Oro, A., Esquej, P., Fernández-Hernández, J., Fraile, E., Garabato, D., García-Lario, P., Gosset, E., Haigron, R., Halbwachs, J.L., Hambly, N.C., Harrison, D.L., Hernández, J., Hestroffer, D., Hodgkin, S.T., Holl, B., Janßen, K., Jevardat de Fombelle, G., Jordan, S., Krone-Martins, A., Lanzafame, A.C., Löffler, W., Marchal, O., Marrese, P.M., Moitinho, A., Muinonen, K., Osborne, P., Pancino, E., Pauwels, T., Recio-Blanco, A., Reylé, C., Riello, M., Rimoldini, L., Roegiers, T., Rybizki, J., Sarro, L.M., Siopis, C., Smith, M., Sozzetti, A., Utrilla, E., van Leeuwen, M., Abbas, U., Ábrahám, P., Abreu Aramburu, A., Aerts, C., Aguado, J.J., Ajaj, M., Aldea-Montero, F., Altavilla, G., Álvarez, M.A., Alves, J., Anders, F., Anderson, R.I., Anglada Varela, E., Antoja, T., Baines, D., Baker, S.G., Balaguer-Núñez, L., Balbinot, E., Balog, Z., Barache, C., Barbato, D., Barros, M., Barstow, M.A., Bartolomé, S., Bassilana, J.L., Bauchet, N., Becciani, U., Bellazzini, M., Berihuete, A., Bernet, M., Bertone, S., Bianchi, L., Binnenfeld, A., Blanco-Cuaresma, S., Blazere, A., Boch, T., Bombrun, A., Bossini, D., Bouquillon, S., Bragaglia, A., Bramante, L., Breedt, E., Bressan, A., Brouillet, N., Brugaletta, E., Bucciarelli, B., Burlacu, A., Butkevich, A.G., Buzzi, R., Caffau, E., Cancelliere, R., Cantat-Gaudin, T., Carballo, R., Carlucci, T., Carnerero, M.I., Carrasco, J.M., Casamiquela, L., Castellani, M., Castro-Ginard, A., Chaoul, L., Charlot, P., Chemin, L., Chiaramida, V., Chiavassa, A., Chornay, N., Comoretto, G., Contursi, G., Cooper, W.J., Cornez, T., Cowell, S., Crifo, F., Cropper, M., Crosta, M., Crowley, C., Dafonte, C., Dapergolas, A., David, M., David, P., de Laverny, P., De Luise, F., De March, R., De Ridder, J., de Souza, R., de Torres, A., del Peloso, E.F., del Pozo, E., Delbo, M., Delgado, A., Delisle, J.B., Demouchy, C., Dharmawardena, T.E., Di Matteo, P., Diakite, S., Diener, C., Distefano, E., Dolding, C., Edvardsson, B., Enke, H., Fabre, C., Fabrizio, M., Faigler, S., Fedorets, G., Fernique, P., Fienga, A., Figueras, F., Fournier, Y., Fouron, C., Fragkoudi, F., Gai, M., Garcia-Gutierrez, A., Garcia-Reinaldos, M., García-Torres, M., Garofalo, A., Gavel, A., Gavras, P., Gerlach, E., Geyer, R., Giacobbe, P., Gilmore, G., Girona, S., Giuffrida, G., Gomel, R., Gomez, A., González-Núñez, J., González-Santamaría, I., González-Vidal, J.J., Granvik, M., Guillout, P., Guiraud, J., Gutiérrez-Sánchez, R., Guy, L.P., Hatzidimitriou, D., Hauser, M., Haywood, M., Helmer, A., Helmi, A., Sarmiento, M.H., Hidalgo, S.L., Hilger, T., Hładczuk, N., Hobbs, D., Holland, G., Huckle, H.E., Jardine, K., Jasniewicz, G., Jean-Antoine Piccolo, A., Jiménez-Arranz, Ó., Jorissen, A., Juaristi Campillo, J., Julbe, F., Karbevska, L., Kervella, P., Khanna, S., Kontizas, M., Kordopatis, G., Korn, A.J., Kóspál, Á., Kostrzewa-Rutkowska, Z., Kruszyńska, K., Kun, M., Laizeau, P., Lambert, S., Lanza, A.F., Lasne, Y., Le Campion, J.F., Lebreton, Y., Lebzelter, T., Leccia, S., Leclerc, N., Lecoeur-Taibi, I., Liao, S., Licata, E.L., Lindstrøm, H.E.P., Lister, T.A., Livanou, E., Lobel, A., Lorca, A., Loup, C., Madrero Pardo, P., Magdaleno Romeo, A., Managau, S., Mann, R.G., Manteiga, M., Marchant, J.M., Marconi, M., Marcos, J., Marcos Santos, M.M.S., Marín Pina, D., Marinoni, S., Marocco, F., Marshall, D.J., Martin Polo, L., Martín-Fleitas, J.M., Marton, G., Mary, N., Masip, A., Massari, D., Mastrobuono-Battisti, A., Mazeh, T., McMillan, P.J., Messina, S., Michalik, D., Millar, N.R., Mints, A., Molina, D., Molinaro, R., Molnár, L., Monari, G., Monguió, M., Montegriffo, P., Montero, A., Mor, R., Mora, A., Morbidelli, R., Morel, T., Morris, D., Muraveva, T., Murphy, C.P., Musella, I., Nagy, Z., Noval, L., Ocaña, F., Ogden, A., Ordenovic, C., Osinde, J.O., Pagani, C., Pagano, I., Palaversa, L., Palicio, P.A., Pallas-Quintela, L., Panahi, A., Payne-Wardenaar, S., Peñalosa Esteller, X., Penttilä, A., Pichon, B., Piersimoni, A.M., Pineau, F.X., Plachy, E., Plum, G., Poggio, E., Prša, A., Pulone, L., Racero, E., Ragaini, S., Rainer, M., Raiteri, C.M., Rambaux, N., Ramos, P., Ramos-Lerate, M., Re Fiorentin, P., Regibo, S., Richards, P.J., Rios Diaz, C., Ripepi, V., Riva, A., Rix, H.W., Rixon, G., Robichon, N., Robin, A.C., Robin, C., Roelens, M., Rogues, H.R.O., Rohrbasser, L., Romero-Gómez, M., Rowell, N., Royer, F., Ruz Mieres, D., Rybicki, K.A., Sadowski, G., Sáez Núñez, A., Sagristà Sellés, A., Sahlmann, J., Salguero, E., Samaras, N., Sanchez Gimenez, V., Sanna, N., Santoveña, R., Sarasso, M., Schultheis, M., Sciacca, E., Segol, M., Segovia, J.C., Ségransan, D., Semeux, D., Shahaf, S., Siddiqui, H.I., Siebert, A., Siltala, L., Silvelo, A., Slezak, E., Slezak, I., Smart, R.L., Snaith, O.N., Solano, E., Solitro, F., Souami, D., Souchay, J., Spagna, A., Spina, L., Spoto, F., Steele, I.A., Steidelmüller, H., Stephenson, C.A., Süveges, M., Surdej, J., Szabados, L., Szegedi-Elek, E., Taris, F., Taylor, M.B., Teixeira, R., Tolomei, L., Tonello, N., Torra, F., Torra, J., Torralba Elipe, G., Trabucchi, M., Tsounis, A.T., Turon, C., Ulla, A., Unger, N., Vaillant, M.V., van Dillen, E., van Reeven, W., Vanel, O., Vecchiato, A., Viala, Y., Vicente, D., Voutsinas, S., Weiler, M., Wevers, T., Wyrzykowski, Ł., Yoldas, A., Yvard, P., Zhao, H., Zorec, J., Zucker, S., Zwitter, T., 2023. Gaia data release 3. Summary of the content and survey properties. Astron. Astrophys. 674, A1. http://dx.doi.org/10.1051/0004-6361/202243940, arXiv:2208.00211.

Gill, D., 1913. History and description of the Royal Observatory Cape of Good Hope. Her Majesty's Stationary Office (HMSO), London.

Ianna, P.A., Seitzer, P.O., 1979. A report on the natural satellite observational program at the university of virginia. In: Nacozy, P.E., Ferraz-Mello, S. (Eds.), Natural and Artificial Satellite Motion. p. 33.

Kostinsky, S., 1908. Photographische beobachtung der bedeckung des sterns B.D.-6.p0s6191 durch den Planeten Jupiter am 19. Sept. 1903. Mitteilungen Nikolai-Hauptsternwarte Pulkowo 2 (23), 221–232.

Lainey, V., Arlot, J.-E., Karatekin, Ö., van Hoolst, T., 2009. Strong tidal dissipation in io and Jupiter from astrometric observations. Nature 459 (7249), 957–959. http://dx.doi.org/10.1038/nature08108.

Lindegren, L., 1980. Atmospheric limitations of narrow-field optical astrometry. Astron. Astrophys. 89 (1–2), 41–47.

McAlister, H.A., Ianna, P.A., Fredrick, L.W., 1974. On the temperature dependence of scale for the 26-in. McCormick refractor. Astron. J. 79, 1445. http://dx.doi.org/10.1086/111698.

Ockert-Bell, M.E., Burns, J.A., Daubar, I.J., Thomas, P.C., Veverka, J., Belton, M.J.S., Klaasen, K.P., 1999. The structure of Jupiter's ring system as revealed by the galileo

imaging experiment. Icarus 138 (2), 188–213. http://dx.doi.org/10.1006/icar.1998.6072.
Pascu, D., 1977. Astrometric techniques for the observations of planetary satellites. In: IAU Colloq. 28: Planetary Satellites. p. 63.
Pascu, D., 1979. The naval observatory program for the astrometric observation of planetary satellites. In: Nacozy, P.E., Ferraz-Mello, S. (Eds.), Natural and Artificial Satellite Motion. p. 17.
Perlbarg, A.C., Desmars, J., Robert, V., Hestroffer, D., 2023. NAROO program. Precovery observations of potentially hazardous asteroids. Astron. Astrophys. 680, A41. http://dx.doi.org/10.1051/0004-6361/202347100.
Refregier, A., 2003. Shapelets - I. A method for image analysis. Mon. Not. R. Astron. Soc. 338 (1), 35–47. http://dx.doi.org/10.1046/j.1365-8711.2003.05901.x, arXiv:astro-ph/0105178.
Robert, V., 2011. Ph.D. thesis, Observatoire de Paris (Ph.D. thesis). ED127,
Robert, V., de Cuyper, J.P., Arlot, J.E., de Decker, G., Guibert, J., Lainey, V., Pascu, D., Winter, L., Zacharias, N., 2011. A new astrometric reduction of photographic plates using the damian digitizer: improving the dynamics of the Jovian system. Mon. Not. R. Astron. Soc. 415 (1), 701–708. http://dx.doi.org/10.1111/j.1365-2966.2011.18747.x.
Robert, V., Desmars, J., Lainey, V., Arlot, J.E., Perlbarg, A.C., Horville, D., Aboudarham, J., Etienne, C., Guérard, J., Ilovaisky, S., Khovritchev, M.Y., Le Poncin-Lafitte, C., Le Van Suu, A., Neiner, C., Pascu, D., Poirier, L., Schneider, J., Tanga, P., Valls-Gabaud, D., 2021. The NAROO digitization center. Overview and scientific program. Astron. Astrophys. 652, A3. http://dx.doi.org/10.1051/0004-6361/202140472.
Robert, V., Pascu, D., Lainey, V., Arlot, J.E., De Cuyper, J.P., Dehant, V., Thuillot, W., 2016. New astrometric measurement and reduction of USNO photographic observations of the main Saturnian satellites: 1974–1998. Astron. Astrophys. 596, A37. http://dx.doi.org/10.1051/0004-6361/201629807.
Robin, A.C., Luri, X., Reylé, C., Isasi, Y., Grux, E., Blanco-Cuaresma, S., Arenou, F., Babusiaux, C., Belcheva, M., Drimmel, R., Jordi, C., Krone-Martins, A., Masana, E., Mauduit, J.C., Mignard, F., Mowlavi, N., Rocca-Volmerange, B., Sartoretti, P., Slezak, E., Sozzetti, A., 2012. Gaia universe model snapshot. A statistical analysis of the expected contents of the Gaia catalogue. Astron. Astrophys. 543, A100. http://dx.doi.org/10.1051/0004-6361/201118646, arXiv:1202.0132.
Seidelmann, P.K., 1979. Planetary satellites, a review of the past and assessment of the future. In: Nacozy, P.E., Ferraz-Mello, S. (Eds.), Natural and Artificial Satellite Motion. p. 3.
Struve, G., 1928. Preliminary results of a comparison between visual and photographic observations of the satellites of Saturn, made in Johannesburg, in 1926. Astron. J. 39, 9–12. http://dx.doi.org/10.1086/104866.
Van De Kamp, P., 1967. Principles of Astrometry. W. H. Freeman and Company, San Francisco.
Zacharias, N., Urban, S.E., Zacharias, M.I., Wycoff, G.L., Hall, D.M., Monet, D.G., Rafferty, T.J., 2004. The second US naval observatory CCD astrograph catalog (UCAC2). Astron. J. 127 (5), 3043–3059. http://dx.doi.org/10.1086/386353, arXiv:astro-ph/0403060.
Zacharias, N., Winter, L., Holdenried, E.R., De Cuyper, J.P., Rafferty, T.J., Wycoff, G.L., 2008. The StarScan plate measuring machine: Overview and calibrations. Publ. Astron. Soc. Pac. 120 (868), 644. http://dx.doi.org/10.1086/589845, arXiv:0806.0256.